MOLECULAR AND CELLULAR BIOLOGY, June 2011, p. 2392–2403 Vol. 31, No. 12
0270-7306/11/$12.00 doi:10.1128/MCB.01218-10

Hepatocyte-Derived Snail1 Propagates Liver Fibrosis Progression▽†

R. Grant Rowe,[1] Yongshun Lin,[1] Ryoko Shimizu-Hirota,[1] Shinichiro Hanada,[2,4] Eric G. Neilson,[5] Joel K. Greenson,[3] and Stephen J. Weiss[1]*

Division of Molecular Medicine and Genetics, Department of Internal Medicine, Life Sciences Institute,[1] Department of Molecular and Integrative Physiology,[2] and Department of Pathology,[3] University of Michigan, Ann Arbor, Michigan 48109; Division of Gastroenterology, Department of Medicine, Kurume University School of Medicine, Kurume, Japan[4]; and Department of Medicine, Vanderbilt University, Nashville, Tennessee 37232[5]

Received 18 October 2010/Returned for modification 26 November 2010/Accepted 31 March 2011

Chronic exposure of the liver to hepatotoxic agents initiates an aberrant wound healing response marked by proinflammatory, as well as fibrotic, changes, leading to compromised organ structure and function. In a variety of pathological states, correlative links have been established between tissue fibrosis and the expression of transcription factors associated with the induction of epithelial-mesenchymal cell transition (EMT) programs similar to those engaged during development. However, the role played by endogenously derived, EMT-associated transcription factors in fibrotic states *in vivo* remains undefined. Using a mouse model of acute liver fibrosis, we demonstrate that hepatocytes upregulate the expression of the zinc finger transcriptional repressor, Snail1, during tissue remodeling. Hepatocyte-specific ablation of Snail1 demonstrates that this transcription factor plays a key role in liver fibrosis progression *in vivo* by triggering the proximal genetic programs that control multiple aspects of fibrogenesis, ranging from growth factor expression and extracellular matrix biosynthesis to the ensuing chronic inflammatory responses that characterize this class of pathological disorders.

Fibrotic liver disease is characterized by changes in tissue architecture and extracellular matrix composition that ultimately compromise organ function (2, 8, 36, 54). Current models of acute liver injury emphasize hepatocyte cell death as a critical initiator of fibrosis by virtue of the ability of the apoptotic/necrotic cells to trigger an inflammatory cascade that serves to recruit resident Kupffer cells, hepatic stellate cells, infiltrating leukocytes, and bone marrow-derived cell populations to the matrix-remodeling program (54). Despite the fact that hepatocytes are the dominant cell type residing in the liver, few studies have considered the possibility that hepatocytes themselves actively orchestrate the fibroproliferative responses that precipitate organ damage (2, 8, 36, 54).

Fibrotic programs affecting multiple organ systems have been shown to correlate with the expression of one or more members of the Snail, ZEB, or Twist family of transcriptional repressors (13, 24, 30, 40, 55, 57). Although expression of these transcription factors is normally restricted to defined periods of embryonic development, certain pathological states are known to trigger their reactivation (25, 49). Nevertheless, despite the fact that epithelial-mesenchymal cell transition (EMT)-promoting transcription factors can be detected in profibrotic states (13, 23, 24, 40), functional roles for any of these endogenously derived molecules during fibrogenesis *in vivo* remain undefined. Here, we demonstrate that liver fibrosis triggers the *in vivo* expression of the zinc finger transcriptional repressor, Snail1. Using a mouse model of hepatocyte-specific Snail1 ablation, this EMT-inducing transcription factor is now identified as a requisite effector of fibrotic progression and the associated inflammatory responses that accompany the disease process.

* Corresponding author. Mailing address: University of Michigan, Life Sciences Institute, 5000 LSI, 210 Washtenaw, Ann Arbor, MI 48109-2216. Phone: (734) 764-0030. Fax: (734) 764-1934. E-mail: SJWEISS@umich.edu.

† Supplemental material for this article may be found at http://mcb.asm.org/.

▽ Published ahead of print on 11 April 2011.

MATERIALS AND METHODS

Mice. *Snail1*^{loxp} mice have been described previously (42). Albumin-Cre transgenic mice and R26R mice (Gtrosa26^{tm1Sor}) were obtained from Jackson Laboratories.

Model of liver fibrosis. Six-week-old male mice were injected in the peritoneum with a 20% solution of carbon tetrachloride (CCl_4) in sterile mineral oil (57). The mice received a dose of 2.5 ml CCl_4 per kilogram of body weight twice per week for 2 weeks. The mice were euthanized 72 h after the final injection. Trichrome-stained liver tissue was scored for liver fibrosis under blinded conditions by two independent investigators, with 5 or more random fields scored and averaged.

Tissue analysis. For the hematoxylin and eosin and Sirius red stains, tissues were fixed in 4% paraformaldehyde and paraffin embedded, sectioned, and stained. For immunofluorescent staining of tissue, fresh liver tissue was frozen in optimal cutting temperature medium and sectioned, fixed with acetone at −20°C for 10 min, and blocked, and primary antibodies were applied overnight. The tissue was then washed with phosphate-buffered saline (PBS), the secondary antibody was applied for 1 to 2 h at room temperature with TOTO-3 counterstain (Invitrogen), and the tissue was washed with PBS and mounted. The antibodies used were rabbit anti-Snail1 (42), rabbit anti-FSP1 (47), mouse anti-albumin (R&D Systems), rabbit anti-collagen I (Abcam), rat anti-CD11b (Serotech), and goat anti-collagen III (Southern Biotechnology). Apoptosis was analyzed with the Roche *in situ* fluorescein cell death detection kit (Roche Diagnostics).

Microscopy and image analysis. Confocal images of cells were acquired on an Olympus FV500 confocal microscope using a 60× water immersion lens with a 1.20 numerical aperture and Fluoview software (Olympus). Collagen deposition was measured by analyzing raw images with MetaMorph software (Molecular Devices).

Microarray analysis of gene expression. Labeled cRNA (generated from RNA) was isolated from three mice for each of four treatment conditions (wild-type [WT] and CKO [see below] mice with and without CCl_4 treatment) or from a Snail1-transduced hepatocyte cell line (see below) and hybridized to mouse 430 2.0 arrays (Affymetrix). Probe signals were transformed into expression values for each gene. Expression values were averaged within each treatment group. When treatment groups were compared, differentially expressed

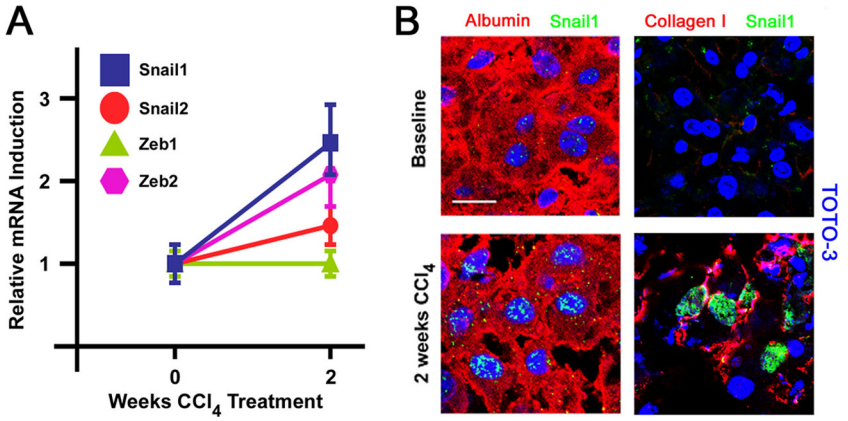

FIG. 1. Snail1 is expressed in response to profibrogenic stimuli. (A) RNA was extracted from uninjured livers or from livers from mice treated with CCl_4 for 2 weeks. The levels of transcripts for Snail1, Snail2, Zeb1, and Zeb2 were analyzed by qRT-PCR. Mean expression values ± SEM for three independent liver samples are presented. (B) Livers were isolated from uninjured mice or mice treated with CCl_4 for 2 weeks. The tissue was sectioned and coimmunostained with antibodies against albumin (red) and Snail1 (green) (left) or collagen I (red) and Snail1 (green) (right). Nuclei were counterstained with TOTO-3 (blue). Scale bar = 20 μm. The results are representative of four separate experiments.

genes were selected, with a fold change cutoff of 2.0 and a *P* value of less than 0.05.

Hepatocyte isolation and culture. Livers were isolated from 6- to 8-week-old male mice, minced, and digested in 0.5 mg/ml collagenase type I (Worthington). The cell suspension was filtered through a 100-μm pore, and the cells were washed and plated on Matrigel (BD Biosciences) with F-12/Dulbecco's modified Eagle's medium (DMEM) (1:1) with 10% fetal bovine serum supplemented with insulin (24). In some experiments, cells were treated with 3 ng/ml recombinant human transforming growth factor β1 (TGF-β1) (R&D Systems). To analyze protein expression, cells were immunostained with mouse monoclonal antibodies against Snail1 (42) or E-cadherin (Zymed Laboratories).

Transgenic expression of Snail1 in hepatocyte lines. AML12 cells were purchased from the American Type Culture Collection (ATCC) and cultured in F12/DMEM (1:1) with 10% fetal calf serum (Invitrogen). Human Snail1 cDNA was subcloned into the FG9 lentiviral expression vector (provided by Colin Duckett, University of Michigan). Recombinant lentivirus was packaged in human embryonic kidney 293 cells (ATCC) and used to infect AML12 cells in the presence of 5 μg/ml Polybrene (Sigma). Expression of exogenous Snail1 was detected by Western blotting to verify expression.

RESULTS

To screen for the expression of EMT-inducing transcription factors during liver fibrosis *in vivo*, mice were chronically treated with the hepatotoxin CCl_4 (57). Following 2 weeks of CCl_4 exposure, expression of hepatic *Snai1* is significantly elevated, as assessed by quantitative RT-PCR (qRT-PCR), with a concomitant, although lesser, induction of the Zeb family member *Zeb2*, with no significant activation of *Snai2* or *Zeb1* (Fig. 1A). Further, other EMT-inducing factors, such as Twist-1, Twist-2, CBF-A, or HMGA2 (49), are not induced, as assessed by cDNA microarray analysis (see the supplemental material).

To confirm the ability of hepatocytes to increase Snail1 protein expression during fibrogenesis, uninjured and fibrotic tissues were double immunostained with a Snail1-specific monoclonal antibody, as well as an antibody directed against mouse albumin, a hepatocyte-specific product (57). As expected, albumin-positive hepatocytes display marked increases in punctate nuclear Snail1 immunoreactivity in fibrotic livers compared to uninjured tissue (Fig. 1B). Further, Snail1-positive cells were detected in association with fibrils of type I collagen deposited during the fibrotic process (Fig. 1B).

In order to characterize the direct consequences of Snail1 induction for hepatocyte function, exogenous Snail1 was expressed in AML12 mouse hepatocytes using a lentiviral system. Snail1-transduced hepatocytes express Snail1, as detected by Western blotting and immunofluorescence microscopy (Fig. 2A and D), and consistent with previous reports (9), Snail1 expression induces a 50% repression of E-cadherin protein and mRNA, indicative of an early EMT process (Fig. 2A and C). Given this functional response, the gene expression profiles of Snail1-expressing and vector control hepatocytes were compared using Affymetrix mouse transcript microarrays. By comparing expression values between Snail1- and vector-transduced cells using significance cutoffs of a minimum 2-fold difference and a *P* value of less than 0.05, 181 differentially expressed distinct genes were identified (see the supplemental material). Consistent with a role for Snail1 in driving a profibrogenic phenotype in hepatocytes, gene ontology (GO) analysis of these genes reveals highly significant enrichment for probe sets annotated as "extracellular space" ($P = 0.000002$), "proteinaceous extracellular matrix" ($P = 0.000006$), and "cell adhesion" ($P = 0.0003$). Among the genes annotated as "proteinaceous extracellular matrix," Snail1 induces expression of transcripts encoding the extracellular matrix proteins collagens I, V, and VI; the proteoglycan versican; and the basement membrane cross-linking protein nidogen 1, as well as lysyl oxidase family members, each of which has been implicated in tissue injury and fibrosis (26, 35, 41) (Fig. 2B). Accordingly, expression of Snail1 in hepatocytes induces expression of *Col1a1* mRNA coincident with an almost 3-fold increase in the deposition of type I collagen fibrils (i.e., 1.0 ± 0.07 arbitrary units [AU] in vector-transduced cells versus 2.7 ± 0.2 AU in Snail1-transduced cells; $P < 0.0001$) (Fig. 2C and D).

A functional role for hepatocyte Snail1 was also assessed *in vitro* by using hepatocytes isolated from $Snai1^{loxp/loxp}$ mice (42). When $Snai1^{loxp/loxp}$ hepatocytes are cultured with TGF-β1, a known signaling mediator of CCl_4-induced liver fibrosis *in vivo* (2, 8, 36, 54), Snail1 mRNA expression is induced 2.8- ± 0.5-fold relative to controls, in combination with clear induction of intranuclear Snail1 staining (Fig. 2E). In contrast, when

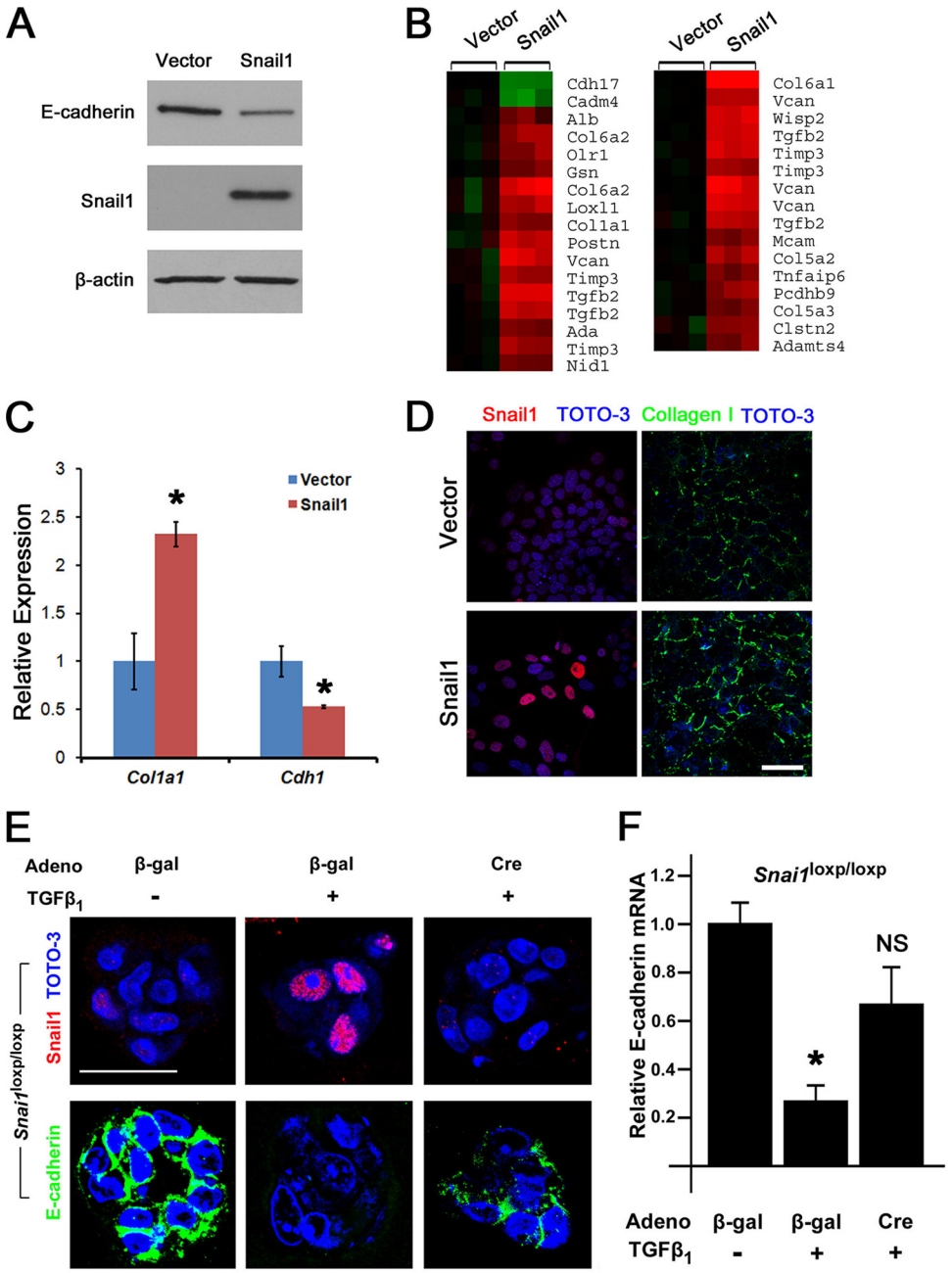

FIG. 2. Snail1 activity in cultured hepatocytes. (A) AML12 cells were transduced with lentiviruses bearing either empty vector or Snail1. Snail1, E-cadherin, and β-actin protein levels were determined by Western blotting. (B) RNA was extracted from vector control or Snail1-expressing AML12 cells and processed for global transcript analysis using Affymetrix microarrays. Differentially expressed genes were analyzed by GO analysis, and a heat map illustrating relative expression levels of genes annotated as "cell adhesion" or "proteinaceous extracellular matrix" is presented. Green denotes Snail1-repressed genes, while red denotes Snail1-induced genes. (C) RNA was isolated from vector- or Snail1-transduced AML12 cells, and the levels ± SEM of the transcripts encoding type I collagen α1 chain and E-cadherin were measured by qRT-PCR (∗, $P < 0.05$). (D) AML12 cells were transduced with lentiviruses encoding empty vector (top) or Snail1 (bottom) and immunostained either for Snail1 after permeabilization (red) (left) or collagen I without permeabilization (green) (right). Scale bar = 50 μm. (E) *Snai1*$^{fl/fl}$ hepatocytes were infected either with a control adenovirus (β-Gal) or a Cre adenovirus and treated with 3 ng/ml TGF-β1 or left untreated for 4 days. Snail1 (red) (top) and E-cadherin (green) (bottom) protein expression was analyzed by immunofluorescent confocal microscopy. Nuclei were counterstained with TOTO-3 (blue). Scale bar = 30 μm. The results are representative of three independent experiments. (F) E-cadherin mRNA levels were analyzed by qRT-PCR ($n = 5$; ∗, $P < 0.0001$; NS, not significant compared to adeno-β-Gal without TGF-β1).

the Snail1^{loxp} allele was recombined *in vitro* by transduction of *Snai1*$^{loxp/loxp}$ hepatocytes with an adenoviral Cre recombinase (adeno-Cre), neither Snail1 mRNA nor protein was detected in response to TGF-β1 treatment (Fig. 2E and data not shown). Further, whereas treatment of control (β-galactosidase [β-Gal]) adenovirus-infected hepatocytes with TGF-β1 results in a marked reduction of expression of the Snail1 target, E-cadherin, at the mRNA and protein levels (49), Snail1-de-

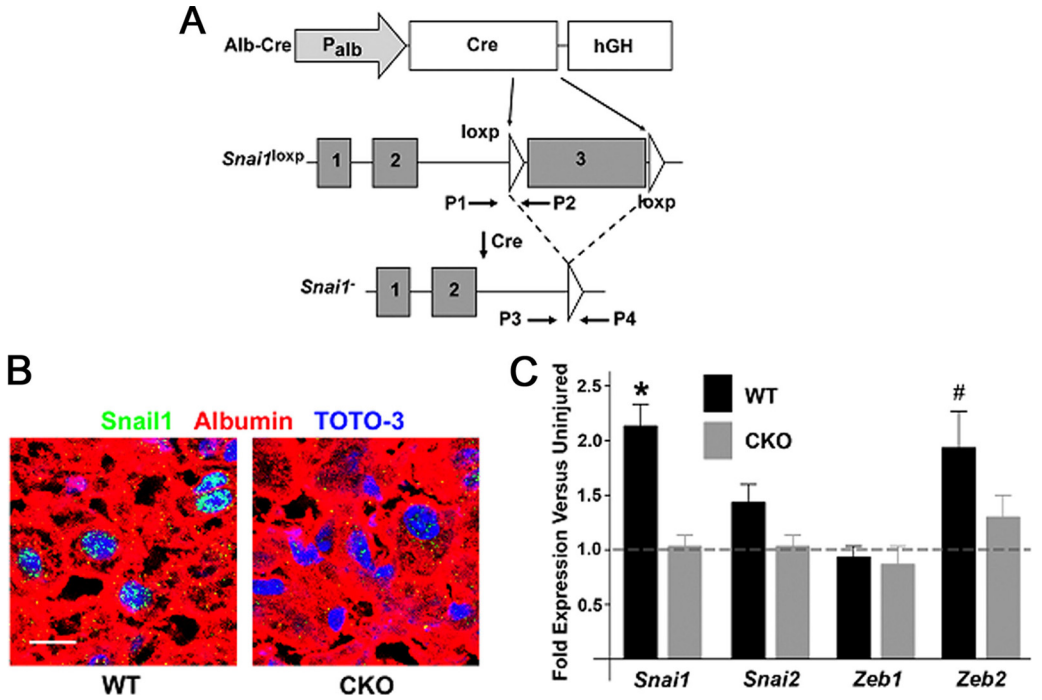

FIG. 3. Targeting Snail1 in hepatocytes *in vivo*. (A) Targeting scheme. Expression of Cre driven by the *Albumin* promoter in hepatocytes excises the *loxp*-flanked third exon of *Snail1*. P1 to P4 indicate positions of PCR primers used for genotyping. (B) Liver tissue was isolated from *Snai1*$^{fl/fl}$ mice (WT) or Alb-Cre *Snai1*$^{fl/fl}$ mice (CKO) and coimmunostained with antibodies against albumin (red) and Snail1 (green), with nuclei counterstained with TOTO-3 (blue). Scale bar = 20 μm. The results are representative of three separate experiments. (C) RNA was isolated from uninjured WT or CKO livers and livers treated with CCl_4 for 2 weeks. qRT-PCR was utilized to measure the expression levels of *Snai1*, *Snai2*, *Zeb1*, and *Zeb2* at baseline and during liver fibrosis. The fold induction and SEM of each gene following CCl_4 treatment for WT and CKO livers is presented (*, $P < 0.05$; #, $P = 0.10$).

ficient adeno-Cre-infected cells are unable to effectively silence E-cadherin expression (Fig. 2E and F). Snail1 silencing does not fully restore E-cadherin expression under these conditions, as TGF-β1 triggers the activation of multiple EMT-inducing factors (50). Nevertheless, these results demonstrate that Snail1 is able to induce an EMT-like program in hepatocytes that is conducive to the expression of a profibrotic phenotype.

To define the role of hepatocyte-derived Snail1 as a profibrogenic agent *in vivo*, *Snai1*^{loxp} mice were crossed with a strain carrying the *Alb-Cre* transgene, where Cre recombinase is expressed under the control of the hepatocyte-specific *Albumin* (*Alb*) promoter to generate *Alb-Cre Snai1*$^{loxp/loxp}$ (here termed CKO) mice (39) (Fig. 3A). Compared to WT (*Snai1*$^{loxp/loxp}$) littermates, CKO mice are viable, display no overt defects, and survive to 6 months and beyond with no ill effects. Importantly, statistically significant changes in gene expression (i.e., using a 2-fold difference and a *P* value of less than 0.05) are not observed between WT and CKO livers, as assessed by whole-genome cDNA microarray analyses (data not shown).

After a 2-week course of CCl_4 treatment, Snail1 protein is detected in hepatocyte nuclei of WT mice, but not in CKO littermates, confirming efficient hepatocyte-specific recombination of the *Snai1*^{loxp} allele without compensatory increases in Snail2, Zeb1, or Zeb2 expression (Fig. 3B and C). Following breeding of CKO mice into the *Rosa26-loxp*-STOP-*loxp-lacZ* (*R26R*) reporter strain, where Cre recombinase also excises the *loxp*-flanked DNA STOP sequence cassette in this allele to activate a β-galactosidase reporter gene in cells containing the functional *Alb-Cre* transgene, staining of liver tissue from *Alb-Cre Snai1*$^{loxp/loxp}$ *R26R* mice and control littermates reveals β-galactosidase activity in >95% of all hepatocytes (Fig. 4). Hence, CKO mouse livers are not populated by Snail1-positive hepatocyte subpopulations as a consequence of selecting cells that have escaped Cre-mediated recombination during liver development.

To determine the functional impact of Snail1 expression on hepatic fibrosis progression, WT and CKO mice were challenged with CCl_4 and changes in liver structure were assessed. CCl_4-treated WT livers display marked increases in the deposition of periportal and interlobular extracellular matrix fibrils rich in collagen types I and III (Fig. 5A and B). In contrast, pathological changes in collagen deposition are attenuated almost completely in CCl_4-treated CKO livers (Fig. 5A and B). In tandem, an attendant decrease is observed in the number of cells expressing fibroblast-specific protein 1 (FSP1), a marker of activated fibroblasts in fibrotic liver (i.e., from 20.8 ± 4.0 cells/high-power field [hpf] [$n = 8$] to 8.3 ± 1.3 [$n = 7$]; $P = 0.02$) (57). Further, using validated criteria to quantify the pathological progression of liver fibrosis, where a score of zero corresponds to a healthy liver (13), fibrosis is reduced significantly in CKO mice compared to WT littermates following CCl_4 treatment ($n = 7$; $P = 0.003$) (Fig. 5C), with no observed differences between the two groups with regard to hepatocyte apoptosis at either day 1 or day 14 post-CCl_4 challenge (1.0 ± 0.2 and 1.3 ± 0.1 for WT versus CKO at 1 day post-CCl_4,

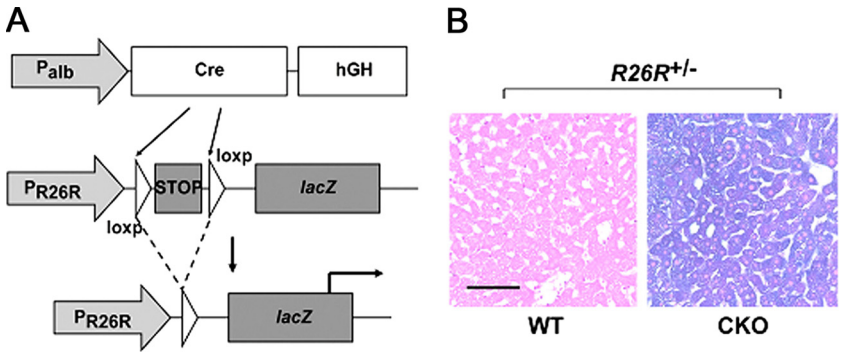

FIG. 4. Hepatocyte-specific *Snai1* deletion verified by the *R26R* reporter strain. (A) CKO mice were bred to the *R26R* reporter strain so that albumin-Cre transgene activity would result in recombination of the *loxp*-flanked STOP cassette in the *R26R* allele, allowing *lacZ* gene expression and β-galactosidase activity in hepatocytes. (B) Liver tissue was isolated from $R26R^{+/-}$ $Snai1^{loxp/loxp}$ mice with or without the albumin-Cre transgene. Whole tissue was stained for β-galactosidase activity (blue), sectioned, and counterstained with eosin, followed by examination by light microscopy. Scale bar = 50 μm.

respectively [$n = 6$], and 1.0 ± 0.4 and 1.4 ± 0.3 for WT versus CKO at 14 days post-CCl_4, respectively [$n = 5$]).

To characterize the mechanisms underlying the role of hepatocyte Snail1 in propagating liver fibrosis, liver tissue mRNA isolated from groups of 3 untreated WT mice, 3 CCl_4-treated WT mice, 3 untreated CKO mice, and 3 CCl_4-treated CKO mice was hybridized to cDNA microarrays for global analysis of transcript expression. Compared to uninjured livers of the corresponding genotype, CCl_4-treated WT livers display significant changes in 1,201 probe sets representing 1,016 unique genes (using a significance cutoff of a P value of 0.05 and a minimum 2-fold change), with GO analysis demonstrating

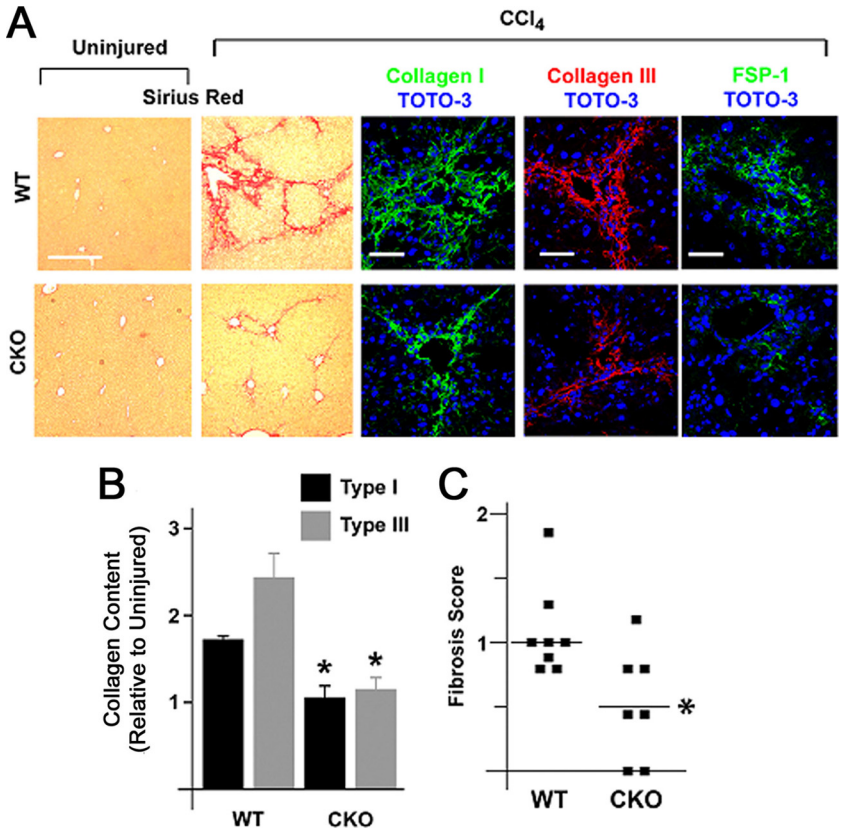

FIG. 5. Hepatocyte Snail1 is required for efficient liver fibrogenesis. (A) Wild-type or CKO mice were treated with CCl_4 for 2 weeks, at which time liver tissue was isolated. The tissue was stained with Sirius red (left two columns; scale bar = 200 μm) or immunostained for collagen I (green; middle column), collagen III (red; fourth column from left), or FSP1 (encoded by the *S100A4* gene) (green; right column) (scale bars = 50 μm) with TOTO-3 counterstaining. (B) Induction of collagen I and III deposition versus uninjured liver was quantified by morphometric analysis ($n = 6$; *, $P < 0.05$). The error bars indicate SEM. (C) Scatter plot demonstrating distribution of fibrosis scores for each genotype (*, $P = 0.003$). Horizontal lines denote mean fibrosis scores.

highly significant enrichment for biological processes related to proliferation ($P = 0.0001$), immune responses ($P = 0.00003$), and inflammation ($P = 0.000001$) (see the supplemental material). In contrast, CKO livers display alterations in a distinctly smaller subset of 634 probe sets representing 558 unique genes versus genotype-matched uninjured livers in response to CCl_4 (see the supplemental material). Analysis of a panel of genes demonstrated previously to contribute directly to the progression of liver fibrosis, including interstitial collagen types I and III (*Col1a1*, *Col1a2*, and *Col3a1*), fibroblast activation markers (fibroblast-specific protein 1 [*FSP1* and *S100a4*], *Vimentin* [*Vim*], and *CD44*], signaling receptors (platelet-derived growth factor receptor β [*Pdgfbr*] and leptin receptor [*Lpr*]), proteases (membrane type I matrix metalloproteinase [*Mmp14*] and cathepsin B [*Ctsb*]), soluble profibrogenic signals (connective tissue growth factor [*Ctgf*] and Sparc), and inflammatory effectors of oxidative stress (*Ncf1* and *Ncf2* subunits of NADPH oxidase) (2, 4, 6, 8, 13, 22, 36, 47, 51, 54), reveals a reduction in activation of these transcripts in CCl_4-treated CKO livers relative to WT livers (Fig. 6C). Decreased expression of a subset of these genes (i.e., *Col1α1*, *Col3α1*, *Snai1*, *S100A4*/*FSP1*, and *Mmp14*) was confirmed by quantitative RT-PCR (data not shown).

Using a minimum 1.5-fold change and a P value of less than 0.05 as significance cutoffs to compensate for the heterogeneity of cell types within livers *in vivo*, genes regulated similarly by CCl_4 *in vivo* and Snail1 in AML12 hepatocytes *in vitro* were identified by merging lists of differentially expressed genes. Using this methodology, 130 probe sets representing 118 distinct genes differentially expressed in both settings were identified, with the observed overlap more significant than expected by random chance ($\chi^2 = 91.0$; $P < 0.0001$) (Fig. 7A) (see the supplemental material). Consistent with its profibrogenic effects in both settings, Snail1 regulates genes encoding the extracellular matrix proteins collagens I, V, and VI and the collagen-cross-linking enzyme lysyl oxidase 1, as well as the proangiogenic factors semaphorin 4D and bone morphogenetic protein endothelial cell precursor-derived regulator (1, 19). GO analysis of these genes revealed further enrichment of genes annotated as extracellular matrix ($P = 3.25 \times 10^{-11}$), proteinaceous extracellular matrix ($P = 1.03 \times 10^{-10}$), extracellular matrix part ($P = 0.0000006$), and basement membrane ($P = 0.00004$) relative to AML12 cells or control liver tissue alone, consistent with a potential role for Snail1 in directing a hepatocyte-autonomous profibrotic program (Fig. 7B).

When differentially expressed probe sets in livers *in vivo* were classified as (i) significantly altered in WT CCl_4-treated livers uniquely, (ii) significantly altered in CKO CCl_4-treated livers uniquely, or (iii) changed in both CCl_4-treated WT and CKO livers relative to baseline genotype-matched controls, GO analysis of each of these gene lists yielded distinct classes of ontology terms for each genotype, with enrichment of terms related to regulation of the immune response in CCl_4-treated WT liver alone and enrichment in terms related to metabolic responses in CKO livers alone (Fig. 6A and B) (see the supplemental material), suggesting that in the absence of hepatocyte Snail1, livers alter metabolic programs in concert with a blunting of the immune response during fibrotic injury. In comparison, gene sets associated with cell cycle regulation and cytokinesis are enriched comparably in both the CCl_4-treated WT and CKO populations (Fig. 6A), results consistent with similar patterns of tissue injury and regeneration in both WT and CKO mice.

Consistent with predicted dampening of the inflammatory response observed in CCl_4-treated CKO tissues, a 2- to 3-log-unit decrease in significance of enrichment of GO terms related to immunity ($P = 0.001$ in CKO versus $P = 0.00003$ in WT) or inflammation ($P = 0.005$ in CKO versus $P = 0.000001$ in WT) is observed in CKO livers relative to WT livers during fibrosis. Corroborating these results, CKO livers display a blunted ability to upregulate genes encoding a panel of proinflammatory mediators linked to mononuclear cell infiltration and function, including platelet-activating factor-acetyl hydrolase (PLA2G7), the B-cell chemokine, CXCL13, leukocyte adhesion molecules, VCAM-1 and ICAM-1, the scavenger receptor CD36, the macrophage marker CD68, and the chemokine receptors CCR2 and CCR5 (Fig. 6D) (12, 20, 37, 44, 45, 54). Furthermore, when hematoxylin- and eosin-stained WT and CKO tissues are compared for changes in leukocyte infiltration, only the fibrotic interstitium of CCl_4-treated WT livers contains multinucleated giant cells (with associated calcifications in 3/8 livers examined), while CKO livers display an altered pattern of inflammation with infiltrates limited to isolated clusters of lymphocyte-like mononuclear cells (Fig. 6E). Accordingly, immunostaining for CD11b, a marker of monocytes and macrophages, is decreased by approximately 50% in CCl_4-treated CKO mice relative to WT controls (i.e., 25 ± 7 CD11b-positive cells/hpf in WT versus 13 ± 2 cells/hpf in CKO mice [mean ± standard error of the mean {SEM}]; $n = 3$) (Fig. 6E). Flow cytometric analysis of leukocyte subpopulations isolated from CCl_4-challenged WT and CKO livers revealed a strong trend of reduced monocytes, F4/80-positive monocyte/macrophages, B cells, and γδ T cells (but not neutrophils or NK cells) in CKO mice, but the changes did not reach statistical significance ($P = 0.13$) due to high variability between samples in each genotype group (data not shown).

To assess the role of endogenous Snail1 in altering the epithelial properties of hepatocytes *in vivo*, tissues were simultaneously immunostained with antibodies against protein markers specific for both differentiated hepatocytes and activated fibroblasts to identify epithelial-like hepatocyte cells actively adopting a "transition state" toward a mesenchymal-cell-like phenotype where epithelial and fibroblast markers are coexpressed, a phenomenon previously observed during liver fibrogenesis *in vivo* (57). Histologic sections of livers were double immunostained with antibodies specific for albumin or E-cadherin in combination with FSP1 and assessed by confocal laser microscopy. Consistent with the observation that hepatocytes are able to initiate EMT-like changes during liver fibrosis (13, 24), FSP1/albumin and FSP1/E-cadherin double-positive cells can be identified in CCl_4-treated, but not uninjured, WT livers (Fig. 8A and B). However, in CCl_4-treated CKO livers, a marked reduction in FSP1/albumin and FSP1/E-cadherin double-positive cells is observed, indicating that Snail1-deficient hepatocytes are resistant to the loss of epithelial cell markers observed in WT hepatocytes in response to hepatotoxic stress *in vivo* (Fig. 8A and B). Though hepatic stellate cells actively propagate fibrotic responses following their transformation into α-smooth muscle actin/Toll-like receptor 4-positive myofibroblasts (2), expression levels of both *Acta2* and *Tlr4* are

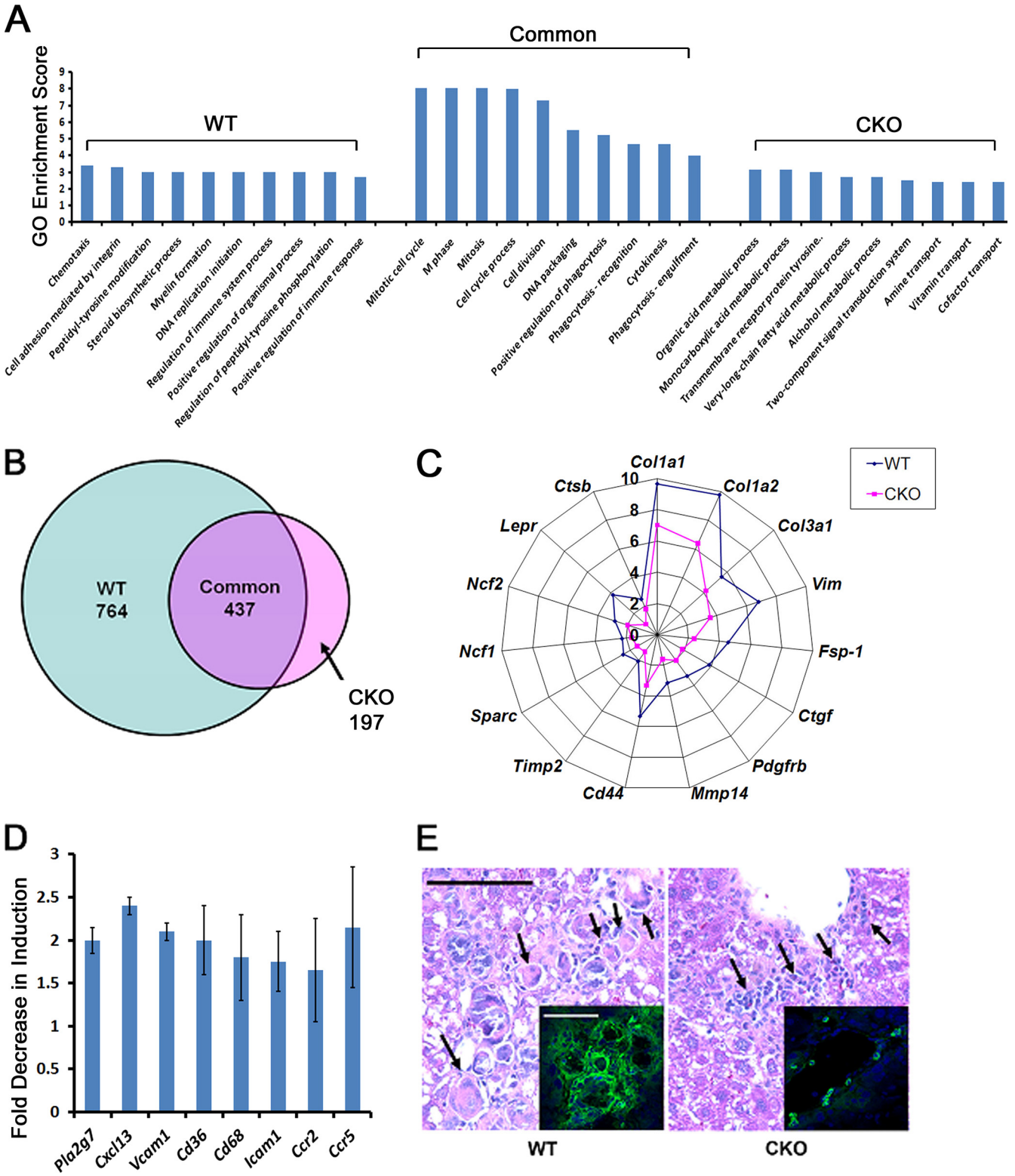

FIG. 6. Induction of Snail1-dependent profibrotic and proinflammatory gene expression programs during hepatic fibrogenesis. (A) RNA was isolated from uninjured livers or from livers from both WT and CKO mice treated with CCl_4 for 2 weeks. Three separate livers were analyzed for both treatment conditions for each genotype. RNA was labeled and hybridized to Affymetrix microarrays for analysis of gene expression, and differentially expressed probe sets were identified for each of the four conditions (significantly changed probe sets were differentially expressed at least 2-fold in CCl_4-treated tissue compared to uninjured tissue; $P \leq 0.05$). The transcripts were classified as significantly altered by CCl_4 in WT livers uniquely or in CKO livers uniquely or altered by CCl_4 in both genotypes (Common). Each of the three groups of probe sets was applied to GO biological process analysis. The GO enrichment scores (negative logarithm of the P value) for the top 10 most significant terms for each probe set group are presented. $n = 3$ livers hybridized for both genotypes and treatment conditions. (B) Venn diagram demonstrating differentially

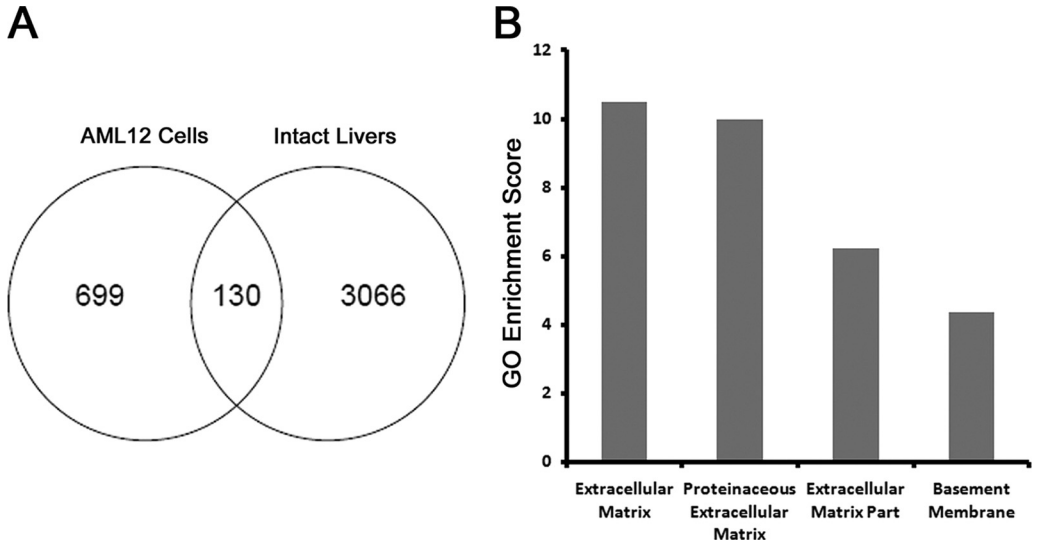

FIG. 7. Identification of a hepatocyte Snail1-regulated transcriptional program. (A) Using significance cutoffs of a minimum 1.5-fold change and a *P* value of 0.05, differentially expressed probe sets within both AML-12 cells and intact livers with and without 2 weeks of CCl_4 treatment were identified. One hundred thirty probe sets representing 118 distinct genes appeared on both gene lists. (B) GO analysis of highly enriched terms among the 130 probe sets within the overlapping region. Significance is expressed as GO enrichment scores ($-\log P$ value).

similar in CCl_4-treated WT and CKO livers (data not shown), with indistinguishable patterns of α-smooth muscle actin staining *in vivo* (Fig. 8C and D), suggestive of comparable degrees of hepatic stellate cell activation. Hence, the specific deletion of hepatocyte-derived Snail1 attenuates fibrotic responses in the absence of direct effects on hepatic stellate cell numbers or activation phenotype.

DISCUSSION

Fibrotic disease states have been associated with changes in epithelial cell behavior, consistent with the engagement of EMT or EMT-like programs that occur in combination with the activation of transcription factors linked previously to developmental EMT programs (2, 8, 13, 24, 30, 36, 40, 54, 55, 57). Nevertheless, to date, the impact of tissue-specific ablation of any endogenously derived, EMT-promoting transcription factor on fibrotic disease progression has not been defined. Consequently, the functional roles assumed by these transcriptional regulators in fibrotic states have remained the subject of controversy (2, 8, 13, 24, 30, 36, 40, 54, 55, 57). Indeed, whereas hepatocyte- or epithelial cell-associated EMT programs have been proposed to play important roles during fibrosis (9, 10, 15–17, 28, 57), a series of recent studies have questioned these conclusions (48, 56). Using sophisticated transgenic-animal models that allow the lineage-specific tracking of collagen-synthesizing cells *in vivo*, Taura and colleagues have reported that hepatocytes do not display mesenchymal characteristics during liver fibrosis in CCl_4-treated mice (48). Likewise, whereas Snail1 overexpression in kidney epithelial cells has been proposed to give rise to fibrotic changes via similar EMT-associated processes (5, 7, 34), studies tracing renal epithelial cell fate have demonstrated that mesoderm-derived pericytes (alternatively named perivascular fibroblasts), rather than epithelial cells, are the major cell type giving rise to type I collagen-producing fibroblasts/myofibroblasts *in vivo* (21, 31). Taken together, these findings confound attempts to predict, *a priori*, the functional impact of endogenous hepatocyte Snail1 in the *in vivo* setting of liver fibrosis. Though current models propose that (i) liver fibrosis arises solely as a consequence of hepatocyte damage and (ii) full-scale EMT programs are not engaged during CCl_4-induced liver fibrosis (2, 48, 54), our findings not only identify endogenous Snail1 as a functionally important profibrotic factor, but also demonstrate that hepatocytes directly and actively orchestrate fibroproliferative disease progression through both cell-autonomous and paracrine mechanisms.

Given current controversies regarding Snail1's ability to trigger fibrosis-associated EMT programs *in vivo*, how can one explain these findings? As demonstrated in our studies, the singular deletion of hepatocyte Snail1 exerts a surprisingly wide-ranging effect on fibrosis progression. By affect-

expressed probe sets for the unique WT and CKO and the common groups. (C) The fold increases in expression levels of selected fibrosis-related genes in response to CCl_4 in both WT and CKO livers were determined. (D) Induction of a panel of genes associated with the inflammatory response in response to CCl_4 in WT and CKO livers was measured by microarray analysis. All eight genes were induced significantly in WT livers, but not CKO livers. The fold decrease ± SEM in induction of expression in CKO livers compared to WT livers is presented for each gene ($P < 0.05$; $n = 3$). (E) Hematoxylin- and eosin-stained tissues from WT and CKO CCl_4-treated mice were examined to assess immune cell infiltration. The arrows indicate multinucleated giant cells in WT tissue (left) and mononuclear cell infiltrates in CKO tissue (right) (scale bar = 50 μm). (Insets) Tissues were stained for CD11b (green) and counterstained with TOTO-3 (blue) (scale bar = 50 μm).

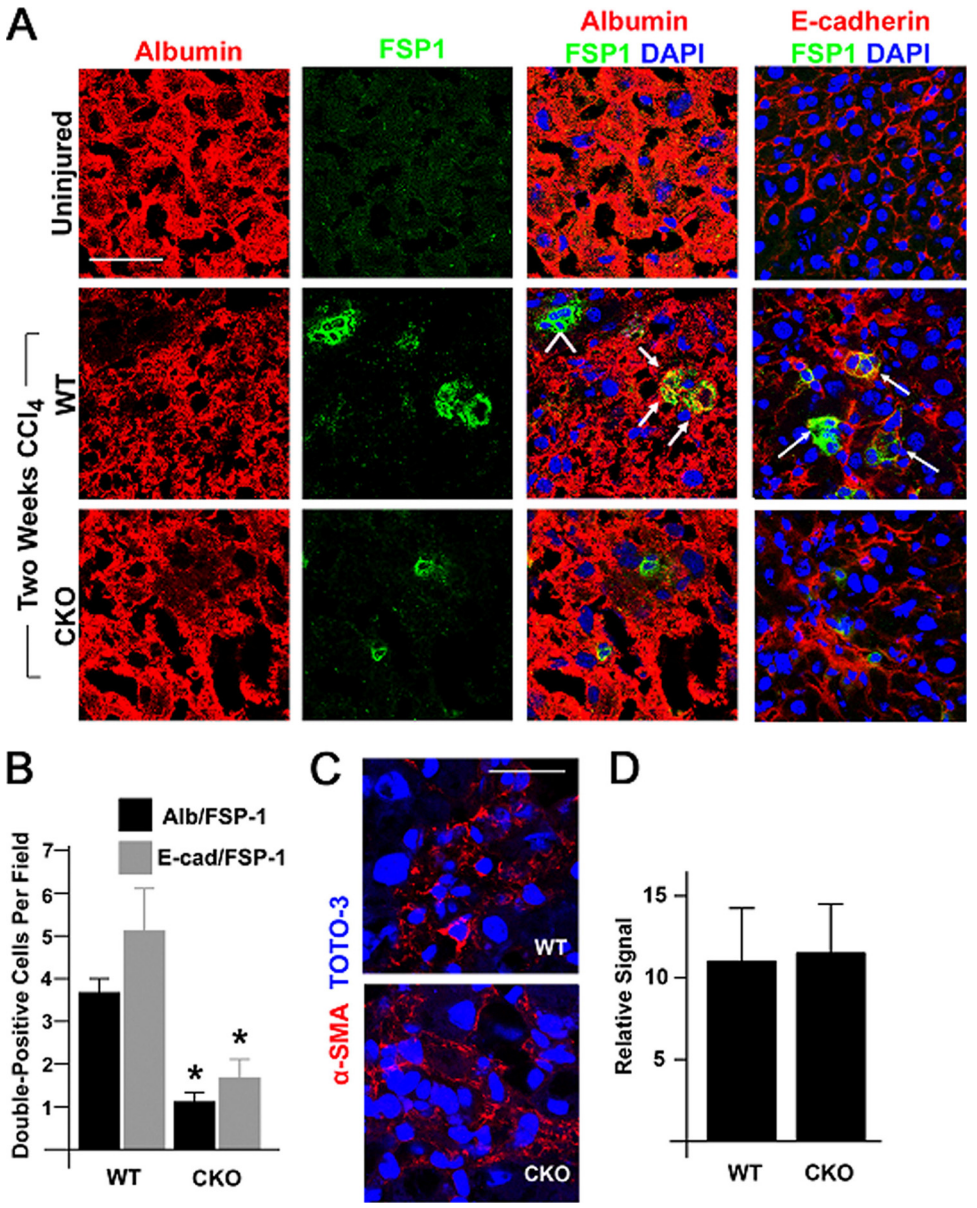

FIG. 8. Snail1-dependent changes in hepatocyte differentiation markers during liver fibrogenesis *in vivo*. (A) Liver tissue was isolated from uninjured mice (top row), WT mice treated with CCl_4 for 2 weeks (middle row), or CKO mice treated with CCl_4 for 2 weeks (bottom row). Frozen sections were coimmunostained with antibodies against albumin (red; left column) and FSP1 (also known as S100A4) (green; second column from left), and nuclei were counterstained with TOTO-3. Albumin/FSP1 double-positive cells are indicated by arrows in the merged confocal images. Albumin-negative, FSP1-positive stellate cells are indicated by an arrowhead (blue; third column from left). Scale bar = 50 μm. Liver tissue was coimmunostained with antibodies against E-cadherin (red; right column) and FSP1 (green), with nuclei counterstained with TOTO-3. E-cadherin/FSP1 double-positive cells are indicated by arrows. (B) The number ± SEM of albumin/FSP1 or E-cadherin/FSP1 double-positive cells per field in WT or CKO livers treated with CCl_4 was determined ($n = 8$; *, $P = 0.001$). (C) CCl_4-treated liver tissue was stained for α-smooth muscle actin (red) and counterstained with TOTO-3 (blue). The tissue was examined by confocal laser microscopy. Scale bar = 30 μm. (D) The relative signals for α-smooth muscle actin in WT and CKO livers were analyzed by morphometric analysis and are presented as mean and SEM ($n = 3$).

ing the expression of growth factors critical to liver fibrosis, (e.g., TGF-β1, CTGF, and platelet-derived growth factor [PDGF]), proteases linked to extracellular matrix turnover (MT1-MMP and cathepsins B and K), the synthesis of multiple connective tissue components (ranging from collagen types I, III, V, and VI to syndecan, SPARC, and biglycan), chemokine-chemokine receptor networks, angiogenic factors (Bmper and Sema4d), and adhesion molecules (2, 8, 36, 54), Snail1 most likely directs profibrotic programs by controlling the expression of multiple signaling cascades that impact hepatocyte, as well as nonhepatocyte cell populations, including hepatic stellate cells, endothelial cells, Kupffer cells, and bone marrow-derived cells (14, 43). Indeed, histologic analyses, coupled with GO analysis of dif-

ferentially expressed transcripts in whole-liver tissue, demonstrate an attenuated CCl_4-induced inflammatory response in the absence of hepatocyte Snail1. Given the fact that selective macrophage depletion confers resistance to CCl_4-induced fibrosis, the profibrogenic effects exerted by Snail1 may be mediated, in part, through changes in the recruitment of mononuclear cells and consequent inflammatory tissue damage (14, 43–45). While links between EMT-associated programs and inflammation are not commonly considered in fibrotic disease, Snail1 has recently been shown to modulate immune responses in neoplastic states (29, 33). Consequently, our findings suggest that the inflammatory cell axis may represent an important component of the intercellular programs triggered by pathological Snail1 activation. At present, however, it is not possible to discriminate between the possibility that a reduction in Snail1 expression decreases inflammation-dependent fibrosis and the possibility that immune cell influx is attenuated as a consequence of a decrease in upstream Snail1-dependent fibrotic events. Nevertheless, in either scenario, Snail1 acts as a key effector of the fibrotic program.

During liver fibrosis, the EMT-promoting factor Zeb2 is concurrently induced, along with the recruitment of Snail1 during fibrosis *in vivo*. Zeb2 is a mediator of neural crest EMT during development (52, 53), and its expression during CCl_4 treatment suggests potential functional cooperation between these two factors during liver fibrogenesis. Interestingly, following Snail1 deletion, a reduction in fibrosis occurs in tandem with a strong trend toward decreased CCl_4-induced Zeb2 induction, a finding consistent with reports characterizing Snail1 as a positive posttranscriptional regulator of Zeb2 mRNA expression (3), suggesting that a similar mechanism may be active during fibrosis *in vivo*. Further investigation into the potential synergy of Snail1 and Zeb2 in contributing to fibrotic events is warranted. However, given the complexity and range of Snail1's field of action during liver fibrosis, it seems naïve to subscribe to the oft-favored notion that a single downstream effector, or pathway, can be identified that will provide an unequivocal "mechanistic basis" for its mode of action *in vivo*. Indeed, in an attempt to dissect the transcriptional basis of Snail1's role in mediating fibrotic responses, we expressed exogenous Snail1 in a mouse hepatocyte line and observed 179 Snail1-regulated transcripts in this simplified model and regulation of genes associated with diverse processes, including extracellular matrix assembly and cell adhesion. Nevertheless, we did observe significant intersection of the gene expression programs regulated by hepatocyte Snail1 *in vivo* and within AML12 hepatocytes *in vitro*, outlining the potential cell-autonomous, profibrogenic impact of Snail1 expression within this cell population.

Though current attention remains focused on Snail1 function in epithelial cells, recent studies demonstrate that Snail1 also acts as a transcriptional regulator of terminally differentiated mesenchymal cells (42). As such, Snail1 likely engages genetic programs in nascent transitioning hepatocytes, as well as mesenchymal cell populations, in paracrine fashion that collaborate to orchestrate fibrosis and inflammatory responses in tandem (2, 8, 36, 54). In view of the fact that our findings are limited to a single, short-term model of fibrosis, further studies are required to determine the relative role of Snail1 versus that of related transcription factors in long-term studies, as well as other models of fibroproliferative disease. For example, recent studies raise the possibility that endogenous Twist, rather than Snail1, plays a dominant role in renal and lung fibrosis (27, 40), though Twist1 may itself induce Snail expression (46). Nevertheless, Snail1 expression has been detected in human fibrotic disease states ranging from virus-induced hepatitis to idiopathic pulmonary fibrosis (11, 13, 23), providing a strong correlative basis for its proposed role as a central effector of fibrotic responses (5, 13).

In spite of the link our studies have established between endogenous hepatocyte-derived Snail1 and liver fibrosis, the ability of Snail1 to initiate a complete EMT program leading to fibroblast/myofibroblast formation during fibrotic events *in vivo* remains unresolved. Even from the perspective of developmental EMT, Thiery and colleagues have argued that Snail1 is unlikely to play an essential role in mesodermal fate specification (49). Rather, Snail1 appears to preferentially regulate morphogenetic programs associated with cell shape, adhesion, and movement (49). As such, it remains possible that the role of Snail1 in fibrosis may be limited to the formation of "metastable" hepatocytes displaying a combination of epithelial and mesenchymal properties that exert a more complex effect on disease progression than was appreciated previously. Consistent with this premise, we and others have documented the ability of hepatocytes to undergo an incomplete EMT characterized by a partial repression of E-cadherin with maintenance of an overall epithelial-like phenotype *in vitro* and *in vivo* (9, 10, 13, 15, 16, 24, 57). Nevertheless, these data fall short of proving that Snail1-expressing hepatocytes contribute directly to scar formation during liver fibrosis by depositing substantive quantities of type I/III collagens *in vivo*, an untested hypothesis that can be clarified only by conditionally deleting the type I collagen gene in hepatocytes alone. Recent efforts to rule out the possibility that hepatocytes participate directly in type I collagen expression during liver fibrosis *in vivo* should be interpreted cautiously, as these conclusions rest on the use of transgenic mice harboring a type I collagen reporter construct designed originally to monitor collagen expression in hepatic stellate cells (48). As such, the ability of this model to recapitulate the expression of the endogenous type I collagen transcript in hepatocytes *in vivo* has not yet been confirmed (32). Indeed, in contrast to these findings, Dooley and colleagues have reported that transferrin-positive hepatocytes coexpress type I collagen and Snail1 in fibrotic human livers (13). While recent studies also conclude that hepatocytes are unable to express FSP1 (38, 48), much of this work relies on the use of paraformaldehyde-fixed tissues for immunohistochemical analyses rather than the fresh-frozen sections used here and elsewhere (48, 57). Furthermore, in the latest work documenting FSP1 expression in inflammatory macrophages, the ability of hepatocytes to express the protein was not tested directly, while FSP1 mRNA was detected in hepatocytes isolated from CCl_4-treated mice (38). These results notwithstanding, it should be stressed that TGF-β1 can trigger type I collagen expression in hepatocytes without inducing FSP1

expression (24). Additional studies will be required to resolve these differences, but efforts to dismiss the possibility that epithelial cells can undergo EMT in fibrotic states should be interpreted cautiously. Indeed, other groups have rigorously documented the ability of alveolar epithelial cells to transition to type I collagen-producing fibroblasts in pulmonary fibrosis models (28). Clearly, such studies provide an important precedent for further analysis of EMT programs in the liver, as well as other target tissues, in fibrotic states. Nevertheless, our findings document a required role for endogenous hepatocyte Snail1 in the evolution of liver fibrosis independent of the magnitude of the hepatocyte EMT program *per se*. The functional importance of endogenously derived Snail1 documented in this study, coupled with recent progress in developing new therapeutics designed to block Snail1 activity *in vivo* (18), underscores the importance of extending these observations to other disease models.

ACKNOWLEDGMENTS

S.J.W. is supported by NIH grant CA116516 and E.G.N. by NIH grant DK-46282. Work performed in this study was also supported by MDRTC Cell and Molecular Biology Core NIH grant P60 DK020572.

We thank B. Omary (University of Michigan) for helpful discussion. We acknowledge A. Willis for assistance with the analysis of microarray data, as well as B. Moore and T. Moore (University of Michigan) for assistance with flow cytometry analyses.

E.G.N. has licensed the anti-FSP1 antibody to Millipore.

REFERENCES

1. **Basile, J. R., K. Holmbeck, T. H. Bugge, and J. S. Gutkind.** 2007. MT1-MMP controls tumor-induced angiogenesis through the release of semaphorin 4D. J. Biol. Chem. **282:**6899–6905.
2. **Bataller, R., and D. A. Brenner.** 2005. Liver fibrosis. J. Clin. Invest. **115:**209–218.
3. **Beltran, M., et al.** 2008. A natural antisense transcript regulates Zeb2/Sip1 gene expression during Snail1-induced epithelial-mesenchymal transition. Genes Dev. **22:**756–769.
4. **Borkham-Kamphorst, E., et al.** 2004. Dominant-negative soluble PDGF-beta receptor inhibits hepatic stellate cell activation and attenuates liver fibrosis. Lab. Invest. **84:**766–777.
5. **Boutet, A., et al.** 2006. Snail activation disrupts tissue homeostasis and induces fibrosis in the adult kidney. EMBO J. **25:**5603–5613.
6. **Canbay, A., et al.** 2003. Cathepsin B inactivation attenuates hepatic injury and fibrosis during cholestasis. J. Clin. Invest. **112:**152–159.
7. **Cheng, J., et al.** 2010. Serum- and glucocorticoid-regulated kinase 1 is up-regulated following unilateral ureteral obstruction causing epithelial-mesenchymal transition. Kidney Int. **78:**668–678.
8. **Choi, S. S., and A. M. Diehl.** 2009. Epithelial-to-mesenchymal transitions in the liver. Hepatology **50:**2007–2013.
9. **Cicchini, C., et al.** 2006. Snail controls differentiation of hepatocytes by repressing HNF4alpha expression. J. Cell Physiol. **209:**230–238.
10. **Copple, B. L.** 2010. Hypoxia stimulates hepatocyte epithelial to mesenchymal transition by hypoxia-inducible factor and transforming growth factor-beta-dependent mechanisms. Liver Int. **30:**669–682.
11. **Dai, C., et al.** 2009. Wnt/{beta}-Catenin signaling promotes podocyte dysfunction and albuminuria. J. Am. Soc. Nephrol. **20:**1997–2008.
12. **De Keyzer, D., et al.** 2009. Increased PAFAH and oxidized lipids are associated with inflammation and atherosclerosis in hypercholesterolemic pigs. Arterioscler. Thromb. Vasc. Biol. **29:**2041–2046.
13. **Dooley, S., et al.** 2008. Hepatocyte-specific Smad7 expression attenuates TGF-beta-mediated fibrogenesis and protects against liver damage. Gastroenterology **135:**642–659.
14. **Duffield, J. S., et al.** 2005. Selective depletion of macrophages reveals distinct, opposing roles during liver injury and repair. J. Clin. Invest. **115:**56–65.
15. **Flier, S. N., et al.** 2010. Identification of epithelial to mesenchymal transition as a novel source of fibroblasts in intestinal fibrosis. J. Biol. Chem. **285:**20202–20212.
16. **Franco, D. L., et al.** 2010. Snail1 suppresses TGF-beta-induced apoptosis and is sufficient to trigger EMT in hepatocytes. J. Cell Sci. **123:**3467–3477.
17. **Godoy, P., et al.** 2010. Dexamethasone-dependent versus -independent markers of epithelial to mesenchymal transition in primary hepatocytes. Biol. Chem. **391:**73–83.
18. **Harney, A. S., et al.** 2009. Targeted inhibition of Snail family zinc finger transcription factors by oligonucleotide-Co(III) Schiff base conjugate. Proc. Natl. Acad. Sci. **106:**13667–13672.
19. **Heinke, J., et al.** 2008. BMPER is an endothelial cell regulator and controls bone morphogenetic protein-4-dependent angiogenesis. Circ. Res. **103:**804–812.
20. **Heller, F., et al.** 2007. The contribution of B cells to renal interstitial inflammation. Am. J. Pathol. **170:**457–468.
21. **Humphreys, B. D., et al.** 2010. Fate tracing reveals the pericyte and not epithelial origin of myofibroblasts in kidney fibrosis. Am. J. Pathol. **176:**85–97.
22. **Ikejima, K., et al.** 2002. Leptin receptor-mediated signaling regulates hepatic fibrogenesis and remodeling of extracellular matrix in the rat. Gastroenterology **122:**1399–1410.
23. **Jayachandran, A., et al.** 2009. SNAI transcription factors mediate epithelial-mesenchymal transition in lung fibrosis. Thorax **64:**1053–1061.
24. **Kaimori, A., et al.** 2007. Transforming growth factor-beta1 induces an epithelial-to-mesenchymal transition state in mouse hepatocytes in vitro. J. Biol. Chem. **282:**22089–22101.
25. **Kalluri, R., and R. A. Weinberg.** 2009. The basics of epithelial-mesenchymal transition. J. Clin. Invest. **119:**1420–1428.
26. **Khan, T., et al.** 2009. Metabolic dysregulation and adipose tissue fibrosis: role of collagen VI. Mol. Cell. Biol. **29:**1575–1591.
27. **Kida, Y., K. Asahina, H. Teraoka, I. Gitelman, and T. Sato.** 2007. Twist relates to tubular epithelial-mesenchymal transition and interstitial fibrogenesis in the obstructed kidney. J. Histochem. Cytochem. **55:**661–673.
28. **Kim, K. K., et al.** 2009. Epithelial cell alpha3beta1 integrin links beta-catenin and Smad signaling to promote myofibroblast formation and pulmonary fibrosis. J. Clin. Invest. **119:**213–224.
29. **Kudo-Saito, C., H. Shirako, T. Takeuchi, and Y. Kawakami.** 2009. Cancer metastasis is accelerated through immunosuppression during Snail-induced EMT of cancer cells. Cancer Cell **15:**195–206.
30. **Lee, J. G., and E. P. Kay.** 2006. FGF-2-mediated signal transduction during endothelial mesenchymal transformation in corneal endothelial cells. Exp. Eye Res. **83:**1309–1316.
31. **Lin, S. L., T. Kisseleva, D. A. Brenner, and J. S. Duffield.** 2008. Pericytes and perivascular fibroblasts are the primary source of collagen-producing cells in obstructive fibrosis of the kidney. Am. J. Pathol. **173:**1617–1627.
32. **Liska, D. J., M. J. Reed, E. H. Sage, and P. Bornstein.** 1994. Cell-specific expression of alpha 1(I) collagen-hGH minigenes in transgenic mice. J. Cell Biol. **125:**695–704.
33. **Lyons, J. G., et al.** 2008. Snail up-regulates proinflammatory mediators and inhibits differentiation in oral keratinocytes. Cancer Res. **68:**4525–4530.
34. **Matsui, I., et al.** 2007. Snail, a transcriptional regulator, represses nephrin expression in glomerular epithelial cells of nephrotic rats. Lab. Invest. **87:**273–283.
35. **Matsumoto, S., et al.** 1999. Immunohistochemical study on phenotypical changes of hepatocytes in liver disease with reference to extracellular matrix composition. Liver **19:**32–38.
36. **Meindl-Beinker, N. M., and S. Dooley.** 2008. Transforming growth factor-beta and hepatocyte transdifferentiation in liver fibrogenesis. J. Gastroenterol. Hepatol. **23:**S122–S127.
37. **Okamura, D. M., et al.** 2009. CD36 regulates oxidative stress and inflammation in hypercholesterolemic CKD. J. Am. Soc. Nephrol. **20:**495–505.
38. **Österreicher, C. H., et al.** 2011. Fibroblast-specific protein 1 identifies an inflammatory subpopulation of macrophages in the liver. Proc. Natl. Acad. Sci. U. S. A. **108:**308–313.
39. **Postic, C., et al.** 1999. Dual roles for glucokinase in glucose homeostasis as determined by liver and pancreatic beta cell-specific gene knock-outs using Cre recombinase. J. Biol. Chem. **274:**305–315.
40. **Pozharskaya, V., et al.** 2009. Twist: a regulator of epithelial-mesenchymal transition in lung fibrosis. PLoS One **4:**e7559.
41. **Rienstra, H., et al.** 2010. Differential expression of proteoglycans in tissue remodeling and lymphangiogenesis after experimental renal transplantation in rats. PLoS One **5:**e9095.
42. **Rowe, R. G., et al.** 2009. Mesenchymal cells reactivate Snail1 expression to drive three-dimensional invasion programs. J. Cell Biol. **184:**399–408.
43. **Russo, F. P., et al.** 2006. The bone marrow functionally contributes to liver fibrosis. Gastroenterology **130:**1807–1821.
44. **Seki, E., et al.** 2009. CCR1 and CCR5 promote hepatic fibrosis in mice. J. Clin. Invest. **119:**1858–1870.
45. **Seki, E., et al.** 2009. CCR2 promotes hepatic fibrosis in mice. Hepatology **50:**185–197.
46. **Smit, M. A., T. R. Geiger, J. Y. Song, I. Gitelman, and D. S. Peeper.** 2009. A Twist-Snail axis critical for TrkB-induced epithelial-mesenchymal transition-like transformation, anoikis resistance, and metastasis. Mol. Cell. Biol. **29:**3722–3737.
47. **Strutz, F., et al.** 1995. Identification and characterization of a fibroblast marker: FSP1. J. Cell Biol. **130:**393–405.

48. **Taura, K., et al.** 2010. Hepatocytes do not undergo epithelial-mesenchymal transition in liver fibrosis in mice. Hepatology **51:**1027–1036.
49. **Thiery, J. P., H. Acloque, R. Y. Huang, and M. A. Nieto.** 2009. Epithelial-mesenchymal transitions in development and disease. Cell **139:**871–890.
50. **Thuault, S., et al.** 2006. Transforming growth factor-beta employs HMGA2 to elicit epithelial-mesenchymal transition. J. Cell Biol. **174:**175–183.
51. **Tong, Z., et al.** 2009. Susceptibility to liver fibrosis in mice expressing a connective tissue growth factor transgene in hepatocytes. Hepatology **50:**939–947.
52. **Van de Putte, T., et al.** 2003. Mice lacking ZFHX1B, the gene that codes for Smad-interacting protein-1, reveal a role for multiple neural crest cell defects in the etiology of Hirschsprung disease-mental retardation syndrome. Am. J. Hum. Genet. **72:**465–470.
53. **Wakamatsu, N., et al.** 2001. Mutations in SIP1, encoding Smad interacting protein-1, cause a form of Hirschsprung disease. Nat. Genet. **27:**369–370.
54. **Wallace, K., A. D. Burt, and M. C. Wright.** 2008. Liver fibrosis. Biochem. J. **411:**1–18.
55. **Zeisberg, E. M., et al.** 2007. Endothelial-to-mesenchymal transition contributes to cardiac fibrosis. Nat. Med. **13:**952–961.
56. **Zeisberg, M., and J. S. Duffield.** 2010. Resolved: EMT produces fibroblasts in the kidney. J. Am. Soc. Nephrol. **21:**1247–1253.
57. **Zeisberg, M., et al.** 2007. Fibroblasts derived from hepatocytes in liver fibrosis via epithelial to mesenchymal transition. J. Biol. Chem. **282:**23337–23347.